



ARCHIVES of FOUNDRY ENGINEERING

ISSN (2299-2944)
Volume 19
Issue 4/2019

91 – 94

10.24425/afe.2019.129636

15/4



Published quarterly as the organ of the Foundry Commission of the Polish Academy of Sciences

The Influence of Riser Shape on Feeding Effectiveness of Solidifying Casting

L. Sowa *, T. Skrzypczak, P. Kwiatóń

Institute of Mechanics and Machine Design Fundamentals, Częstochowa University of Technology
Dąbrowskiego 73, 42-200 Częstochowa, Poland

* Corresponding author. E-mail address: sowa@imipkm.pcz.pl

Received 02.07.2019; accepted in revised form 17.09.2019

Abstract

The mathematical model and numerical simulations of the solidification of a cylindrical shaped casting, which take into account the process of filling the mould cavity by liquid metal and feeding the casting through the riser during its solidification, are presented in the paper. Mutual dependence of thermal and flow phenomena were taken into account because have an essential influence on solidification process. The effect of the riser shape on the effectiveness of feeding of the solidifying casting was determined. In order to obtain the casting without shrinkage defects, an appropriate selection of riser shape was made, which is important for foundry practice. Numerical calculations of the solidification process of system consisting of the casting and the conical or cylindrical riser were carried out. The velocity fields have been obtained from the solution of momentum equations and continuity equation, while temperature fields from solving the equation of heat conductivity containing the convection term. Changes in thermo-physical parameters as a function of temperature were considered. The finite element method (FEM) was used to solve the problem.

Keywords: Solidification process, Castings defects, Numerical simulation, Liquid metal flow

1. Introduction

The growing requirements regarding the quality of castings require intensive technological development of foundry methods, which requires various researches. These studies focus mainly on obtaining castings without shrinkage defects with high mechanical properties through appropriate control of their feeding [1-4] or design of layer castings that are resistant to corrosion or have high heat resistance [5]. Conducting research on real objects is significantly difficult due to the lack of visibility and high temperatures taking place there, which is why only computer simulations make it possible to improve casting methods [6-11]. In this article, the process of casting solidification is analyzed, considering the phenomena of heat exchange and fluid flow, starting from the moment of filling the metal mould by molten metal and ending with the complete solidification of the casting.

The shape of the solidus line is observed, assessing whether it has been closed in the casting area. Such a situation would mean the lack of supply of this area by the liquid metal from the riser and the formation of defects at this place of the casting. We try to avoid this situation by selecting the right shape of riser to the considered casting. Therefore, the aim of the work was to assess the correctness of the shape selection of riser for the solidifying casting, so that it arises without defects.

2. The mathematical description

The superheated metals alloys in the liquid state can be treated as the viscous incompressible fluids [7, 9]. The mathematical description of the casting solidification process considering the liquid metal movements is based on the solution

of the following equations system in a cylindrical axial-symmetric coordinate system [7-11]

– the momentum equations

$$\mu \left(\frac{\partial^2 v_r}{\partial r^2} + \frac{1}{r} \frac{\partial v_r}{\partial r} + \frac{\partial^2 v_r}{\partial z^2} - \frac{v_r}{r^2} \right) - \frac{\partial p}{\partial r} + \rho g_r + \rho g_r \beta (T - T_\infty)_r = \rho \frac{dv_r}{dt},$$

$$\mu \left(\frac{\partial^2 v_z}{\partial r^2} + \frac{1}{r} \frac{\partial v_z}{\partial r} + \frac{\partial^2 v_z}{\partial z^2} \right) - \frac{\partial p}{\partial z} + \rho g_z + \rho g_z \beta (T - T_\infty)_z = \rho \frac{dv_z}{dt},$$
(1)

– the continuity equation

$$\frac{\partial v_r}{\partial r} + \frac{v_r}{r} + \frac{\partial v_z}{\partial z} = 0,$$
(2)

– the equation of heat conductivity with the convection term

$$\frac{\lambda}{r} \frac{\partial T}{\partial r} + \frac{\partial}{\partial r} \left(\lambda \frac{\partial T}{\partial r} \right) + \frac{\partial}{\partial z} \left(\lambda \frac{\partial T}{\partial z} \right) = \rho C_{ef} \frac{\partial T}{\partial t} + \rho C_{ef} \left(v_r \frac{\partial T}{\partial r} + v_z \frac{\partial T}{\partial z} \right),$$
(3)

– the volume fraction equation

$$\frac{\partial F}{\partial t} + v_r \frac{\partial F}{\partial r} + v_z \frac{\partial F}{\partial z} = 0,$$
(4)

where: λ - the thermal conductivity coefficient [W/(mK)], T - the temperature [K], $\rho = \rho(T)$ - the density [kg/m³], $\mu(T)$ - the dynamical viscosity coefficient [kg/(ms)], v_r, v_z - the r -component and z -component of velocity, respectively [m/s], $C_{ef} = c + L/(T_L - T_S)$ - the effective specific heat of a mushy zone [J/(kgK)], t - the time [s], L - the latent heat of solidification [J/kg], g_r, g_z - the r - and z -component of gravitational acceleration, respectively [m/s²], p - the pressure [N/m²], β - the volume coefficient of thermal expansion [1/K], c - the specific heat [J/(kgK)], r, z - the coordinates of the vector of the considered node's position [m], r - the radius [m], T_∞ - the reference temperature ($T_\infty = T_{in}$) [K], F - the pseudo-concentration function across the elements lying on the free surface.

The velocity and pressure fields were obtained from the solution of momentum equations (1) and continuity equation (2), while temperature fields from solving the equation of heat conductivity with the convection term (3). The predicting the filling behaviours of molten metal and the free surface movement is described by the first order pure advection equation (4). In the applied model of solid phase growth, the internal heat source is not visible in the heat conduction equation (3) because it is considered in the effective specific heat of two-phase area [9-11].

The equations (1-4) are completed by appropriate boundary conditions and initial conditions. The initial conditions for temperature and velocity fields are given as [9-11]

$$\mathbf{v}(r, z, t_0) = \mathbf{v}_0(r, z) = v_{in} \Big|_{\Gamma_{1-1}},$$

$$T(r, z, t_0) = T_0(r, z) = \begin{cases} T_{in} & \text{on } \Gamma_{1-1} \\ T_A & \text{in } \Omega_A \\ T_M & \text{in } \Omega_M \end{cases}$$
(5)

The boundary conditions, specified in the considered problem, on the indicated surfaces (Fig. 1), were as follows

– for velocity [9-10]

$$v_n \Big|_{\Gamma_{1-1}} = v_{in}, \quad v_t \Big|_{\Gamma_{1-1}} = v_t \Big|_{\Gamma_{2-2}} = v_n \Big|_{\Gamma_{2-2}} = 0, \quad v_n \Big|_{r=0} = 0,$$
(6)

$$\frac{\partial v_t}{\partial n} \Big|_{r=0} = 0, \quad v_n \Big|_{\Gamma_G} = 0, \quad v_t \Big|_{\Gamma_G} = 0,$$

– for temperature [9-11]

$$T \Big|_{\Gamma_{1-1}} = T_{in}, \quad \lambda_M \frac{\partial T_M}{\partial n} \Big|_{\Gamma_M} = -\alpha_M (T_M \Big|_{\Gamma_M} - T_a),$$

$$\frac{\partial T}{\partial n} \Big|_{\Gamma_{2-2}} = 0, \quad \lambda_S \frac{\partial T_S}{\partial n} \Big|_{\Gamma_{G-}} = \lambda_G \frac{\partial T_G}{\partial n} \Big|_{\Gamma_{G-}},$$
(7)

$$\frac{\partial T}{\partial n} \Big|_{r=0} = 0, \quad \lambda_G \frac{\partial T_G}{\partial n} \Big|_{\Gamma_{G+}} = \lambda_M \frac{\partial T_M}{\partial n} \Big|_{\Gamma_{G+}},$$

where: T_a - the ambient temperature [K], α_M - the heat transfer coefficient between the ambient and the mould [W/(m²K)], T_A - the temperature of air inside mould cavity in initial state [K], T_{in} - the initial temperature [K], T_M, T_G, T_S - the temperature of mould, gap (protective coating) and solid phase, respectively [K], v_{in} - the initial velocity [m/s], $\lambda_M, \lambda_S, \lambda_G$ - the thermal conductivity coefficient of mould, solid phase and gap, respectively [W/(mK)], n - the outward unit normal surface vector, v_t, v_n - the tangential and normal component of velocity vector, respectively [m/s].

3. Example of numerical calculations

To analyse the impact of the movements of the liquid metal alloy and the riser shape on solidification of the casting, the following casting-mould system was considered (Fig. 1). The external mould dimensions were taken as: $d = 0.320$ m, $h = 0.280$ m, while the mould cavity dimensions are equal to: $d_o = 0.200$ m, $h_o = 0.070$ [m], $h_n = 0.150$ m, $d_{nd} = 0.080$ m, $d_{ng} = 0.100$ m, $d_{in} = 0.020$ m. The internal surface of the steel mould is coated by a protective shell with 2mm thickness. The numerical calculations were carried out for the casting made of low-carbon cast steel and the steel mould with thermo-physical properties that were taken from the papers [10, 11]. The overheated metal with temperature $T_{in} = 1850$ K was poured with the velocity $v_{in} = 0.1$ m/s into the steel

mould with initial temperature $T_M=350\text{K}$. Additional important temperatures were equal to: $T_A=350\text{K}$, $T_q=300\text{K}$. The heat transfer coefficient (α) between ambient and the mould was equal $\alpha_M=200\text{W}/(\text{m}^2\text{K})$.

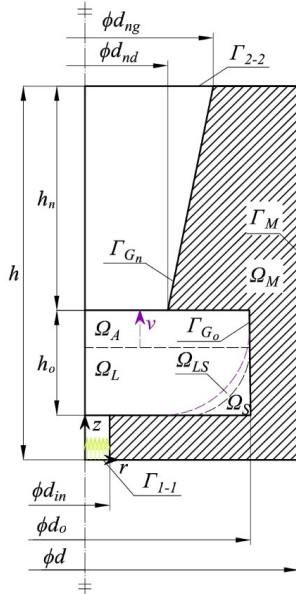


Fig.1. Considered system and identification of regions

Numerical analysis of the solidification process of the casting-riser system was carried out using the given system of equations, which was saved in the FEM with the weighted residuals formulation. The calculations were made for two riser shapes: conical (I variant) or cylindrical (II variant). The main difference between variants I and II rely in the shape of the riser. The possibility of reducing material consumption per riser was assessed, while maintaining its functionality for feeding the casting. For the numerical simulations, the professional Fidap program was used. The geometry of considered system was divided into 4979 quadrilateral finite elements.

4. Analysis of results

Numerous numerical simulations were carried out to determine whether the riser shape was adequately selected to ensure the directional course of the solidification process. The shape of the solidus line was observed in the pictures of temperature distribution, in the subsequent periods of solidification of the casting-riser system, for two variants of the riser shape (Figs 2-5). Comparison of temperature fields in a selected time step, for both variants of the riser shape, is shown in Figure 2b and 3. There is indicated by the solidus line shape for a different manner of cooling these risers. However, Fig. 2a shows an example velocity field corresponding to these temperature fields. If the solidus line closes, the area limited by it will not be fed by liquid metal and a shrinkage defect will occur at this place. If such an area is formed in the casting, it will be defective. We

try to avoid such a situation and move such a defect to the riser by choosing the appropriate shape of riser.

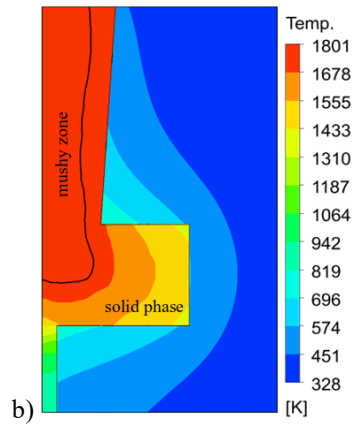
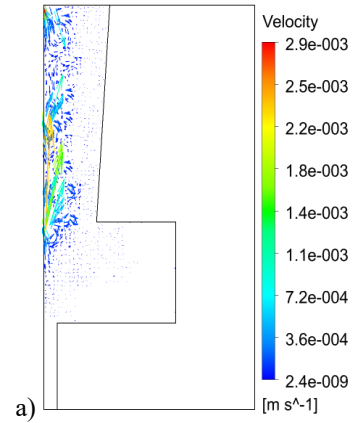


Fig.2. The velocity vectors (a) and temperature distribution (b) at $t=450\text{s}$, I variant

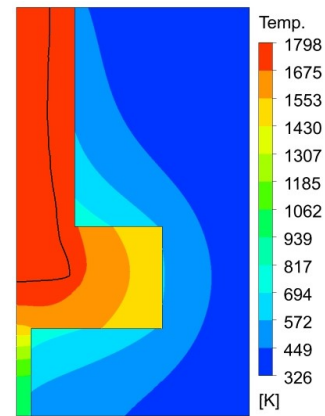


Fig.3. Temperature distribution at $t=450\text{s}$, II variant

When the conical riser was used (Fig. 4), the solidus line left the casting area and the end of solidification took place in the riser. It is estimated that in this case the casting remains free from shrinkage defects. When the cylindrical riser was used (Fig. 5), the solidus line could not leave the upper part of the casting,

suggesting the formation of a shrinkage defect at this place. Therefore, the dimensions of the cylindrical riser should be increased, so that it can fulfil its task.

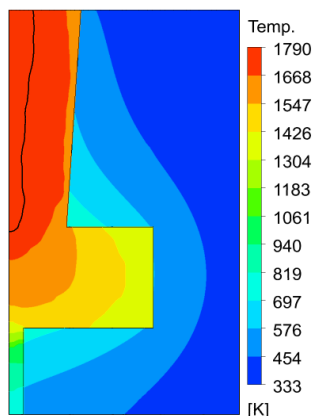


Fig.4. Temperature distribution after solidification of the casting:
 $t=560s$, I variant

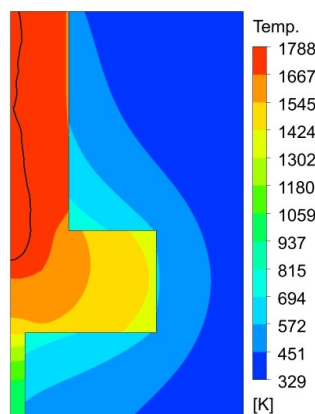


Fig.5. Temperature distribution after solidification of the casting:
 $t=530s$, II variant

5. Conclusions

The mathematical model and numerical simulation results of the casting solidification about a cylindrical shaped, which include the filling process of the mould cavity by molten metal were presented in this paper. The numerical calculations of the casting solidification process were made for two variants depending on assumed of the riser shape. The influence of molten metal motions on the solidification kinetics and the location of shrinkage cavities at the final phase of the casting solidification process were evaluated. It was observed that the solidification process starts effectively after the mould cavity is totally filled by liquid metal. Whereas, in the end solidification stage of the system of casting-riser, the solidus line closed in the upper part of the casting can be seen and thus the position of the shrinkage cavity in this place, when casting process was made using the cylindrical riser (Fig. 5). This phenomenon was not observed if

casting process was made using the conical riser (Fig. 4). In this case, the solidification end took place in the riser, which is wanted, because the riser will be separated and re-processed. It also proves that the conical-shaped riser executed its task and the resulting product is free from casting defects.

References

- [1] Perzyk, M., Kochański, A., Mazurek, P. & Karczewski K. (2014). Selected principles of feeding systems design: simulation vs industrial experience. *Archives of Foundry Engineering*. 14(4), 77-82.
- [2] Nimbulkar, S.L. & Dalu R.S. (2016). Design optimization of gating and feeding system through simulation technique for sand casting of wear plate. *Perspectives in Science*. 8, 39-42. DOI: <https://doi.org/10.1016/j.pisc.2016.03.001>.
- [3] Nadolski, M., Zyska, A., Konopka, Z., Łągiewka, M. & Karolczyk J. (2011). The assessment of bell casting producibility based on computer simulation of pouring and solidification. *Archives of Foundry Engineering*. 11(3), 141-144.
- [4] Cholewa, M. & Szuter T. (2013). Shape complicated casting defects prediction based on computer simulation. *Archives of Metallurgy and Materials*. 58(3), 859-862. DOI: <https://doi.org/10.2478/amm-2013-0087>.
- [5] Szajnar, J., Wróbel, T. & Dulcka A. (2017). Manufacturing methods of alloy layers on casting surfaces. *Journal of Casting & Materials Engineering*. 1(1), 2-6. DOI: doi.org/10.7494/jcme.2017.1.1.2.
- [6] Jezierski, J., Dojka, R. & Janerka K. (2018). Optimizing the gating system for steel castings. *Metals*. 8(4), 266. DOI: doi.org/10.3390/met8040266.
- [7] Huang, P.H. & Lin C-J. (2015). Computer-aided modeling and experimental verification of optimal gating system design for investment casting of precision rotor. *International Journal of Advanced Manufacturing Technology*. 79(7-8), 997-1006. DOI: [10.1007/s00170-015-6897-5](https://doi.org/10.1007/s00170-015-6897-5).
- [8] Huang, P.H., Kuo, J.K., Fang, T.H. & Wu W. (2018). Numerical simulation and design of casting system for stainless steel exhaust manifold. *MATEC Web of Conferences*. 185. DOI: [10.1051/mateconf/201818500008](https://doi.org/10.1051/mateconf/201818500008).
- [9] Dyja, R., Gawrońska, E. & Grosser A. (2018). A computer simulation of solidification taking into account the movement of the liquid phase. *MATEC Web of Conferences*. 157. DOI: [10.1051/mateconf/201815702008](https://doi.org/10.1051/mateconf/201815702008).
- [10] Sowa, L., Skrzypczak, T. & Kwiaton P. (2019). Computer evaluation of the influence of liquid metal movements on defects formation in the casting. *MATEC Web of Conferences*. 254. DOI: [10.1051/mateconf/201925402017](https://doi.org/10.1051/mateconf/201925402017).
- [11] Skrzypczak, T., Węgrzyn-Skrzypczak, E. & Sowa L. (2018). Numerical modeling of solidification process taking into account the effect of air gap. *Applied Mathematics and Computation*. 321, 768-779. DOI: [10.1016/j.amc.2017.11.023](https://doi.org/10.1016/j.amc.2017.11.023).